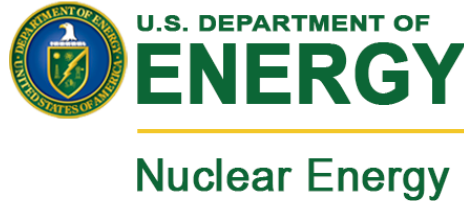


2013 DOE-NEET-3

Stress-strain response of metallic materials via spherical nanoindentation

Jordan Weaver, Cheng Sun, Andrew Nelson, Yongqiang Wang, Nathan Mara
LANL

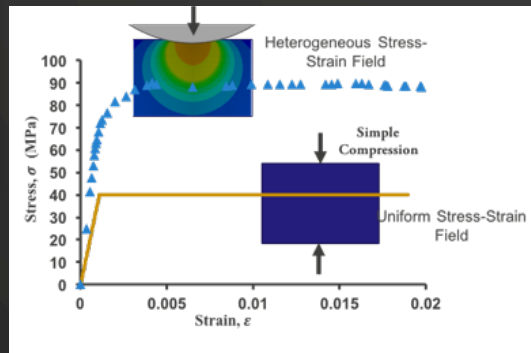
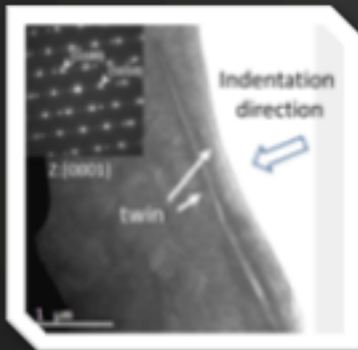
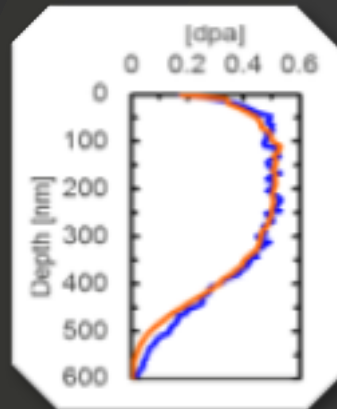
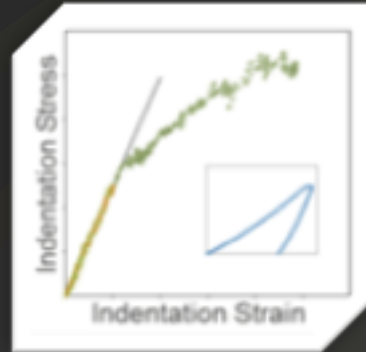
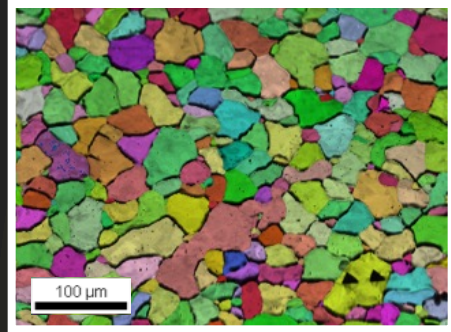


Siddhartha (Sid) Pathak,
University of Nevada, Reno
Dipen Patel, Surya Kalidindi
Georgia Tech



NEET Webinar
August 16th, 2016

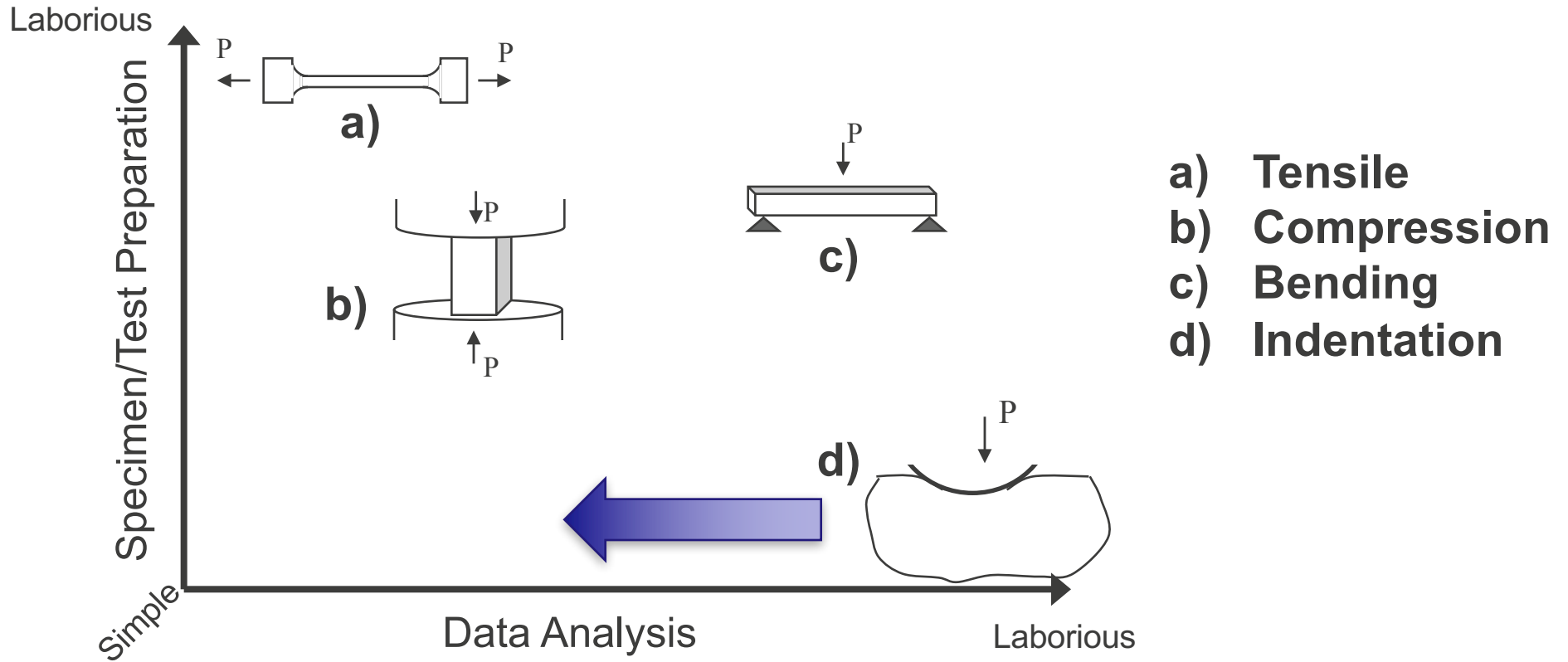
Collaborators: Ashley Reichardt, Peter Hosemann (UC Berkeley)



Outline

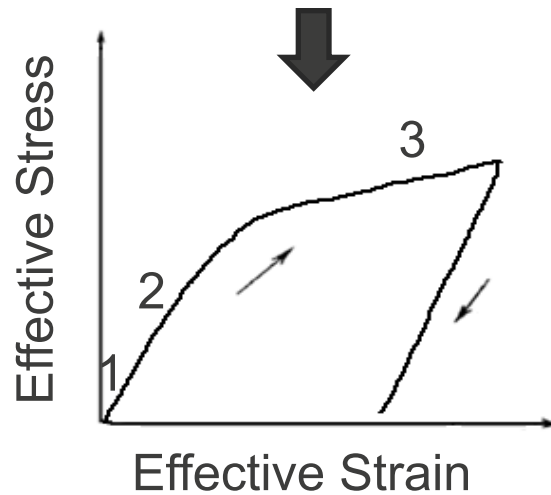
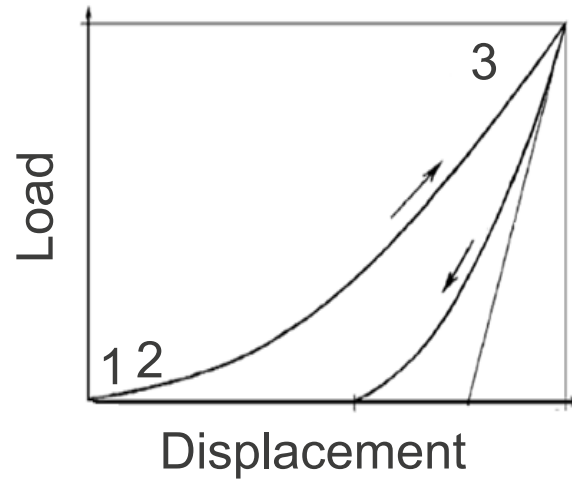
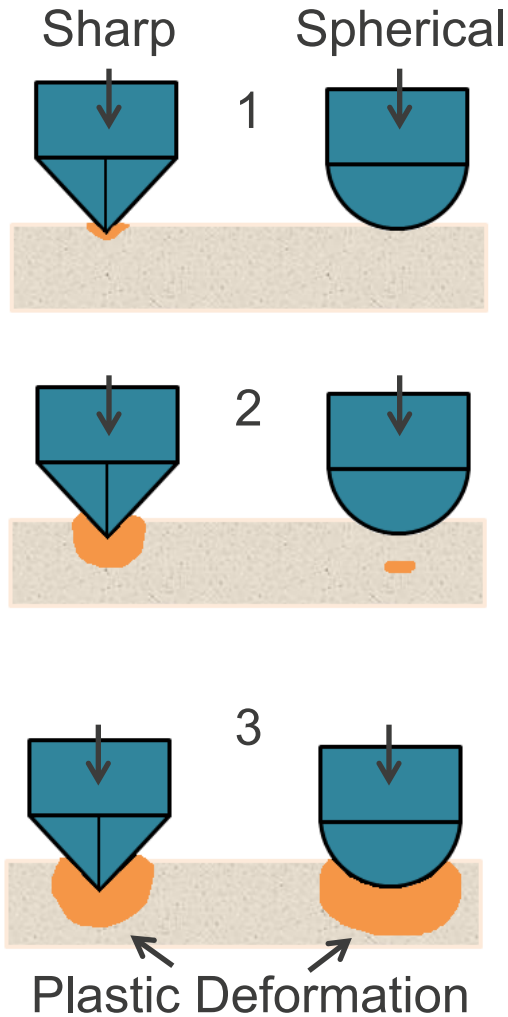
- Spherical nanoindentation stress-strain curves
- Topic I: Ion-irradiated W, 304SS
- Topic II: HCP Zirconium
- Topic III: Correlating Indentation Stress-Strain to Uniaxial Deformation

Mechanical characterization of materials is laborious



Spherical Nanoindentation

Spherical tips are the logical choice



- Capture the response throughout the deformation process.
- Effective stress-strain response.
- Capture the initial elastic response and the elastic-plastic transition.

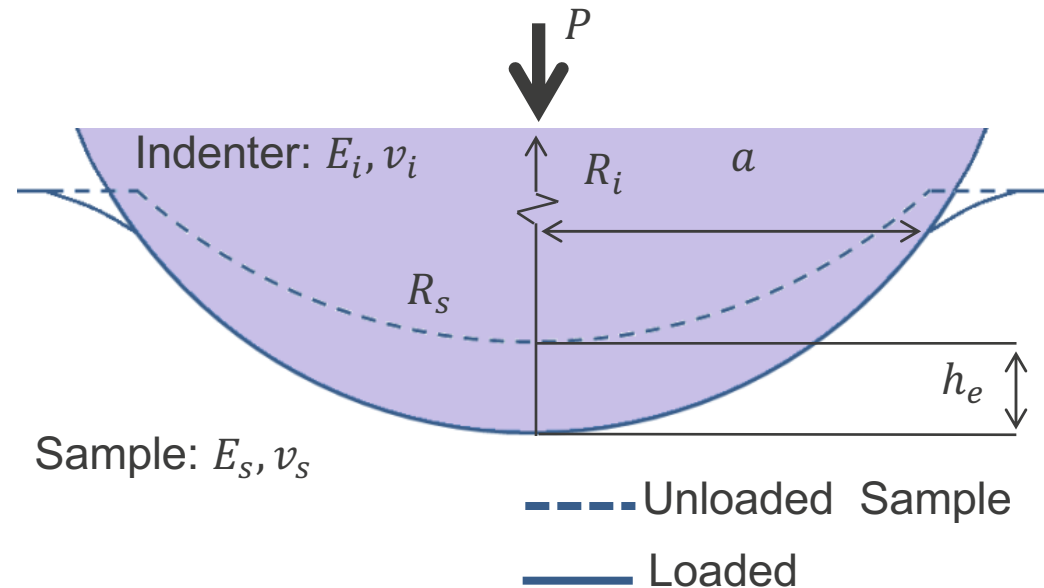
Spherical indentation is well described by Hertz's Theory

$$P = \frac{4}{3} E_{eff} R_{eff}^{\frac{1}{2}} h_e^{\frac{3}{2}}$$

$$a = \sqrt{R_{eff} h_e}$$

$$\frac{1}{E_{eff}} = \frac{1 - \nu_i^2}{E_i} + \frac{1 - \nu_s^2}{E_s}$$

$$\frac{1}{R_{eff}} = \frac{1}{R_i} + \frac{1}{R_s}$$



P, h : load and displacement

a : contact radius

E_{eff}, R_{eff} : effective modulus and radius

E, ν : Young's modulus and Poisson ratio

*Assumptions: (1) isotropic materials, (2) elastic loading or unloading, (3) frictionless contact, (4) quadratic surfaces (e.g., perfect sphere and flat surface).

The load-displacement curve can be converted to an indentation stress-strain (ISS) curve

$$P = \frac{4}{3} E_{eff} R_{eff}^{\frac{1}{2}} h_e^{\frac{3}{2}}$$

$$S = \frac{dP}{dh_e} = 2aE_{eff}$$

$$\sigma_{ind} = \frac{P}{\pi a^2}$$

$$\varepsilon_{ind} = \frac{4h}{3\pi a}$$

S : elastic unloading stiffness

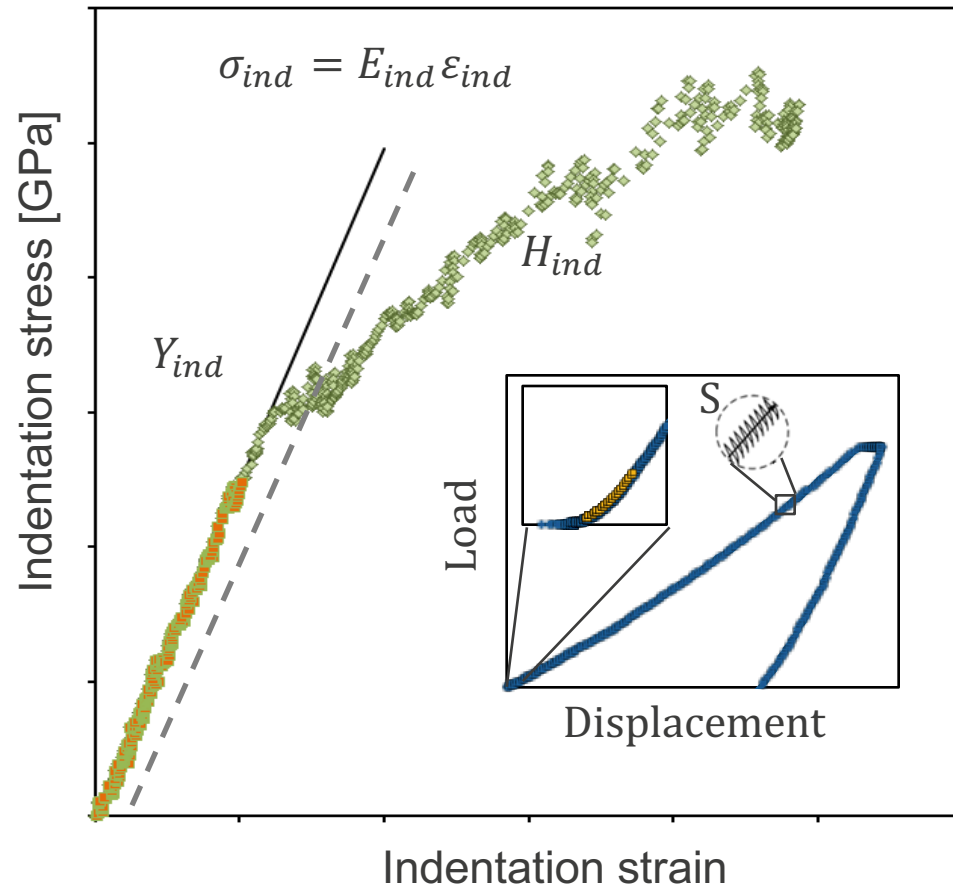
σ_{ind} : indentation stress

ε_{ind} : indentation strain

E_{ind} : indentation modulus

Y_{ind} : indentation yield strength

H_{ind} : indentation work hardening



The new definition of indentation strain is more physically meaningful

$$(A) \quad \varepsilon_{ind} = \frac{4}{3\pi} \frac{a}{R_i}, \quad a = \sqrt{2h_c R_i - h_c^2}$$

D. Tabor The Hardness of Metals. 1951.

Field and Swain JMR, 1993 and 1995.

E. G. Herbert et al. Thin Solid Films, 2001.

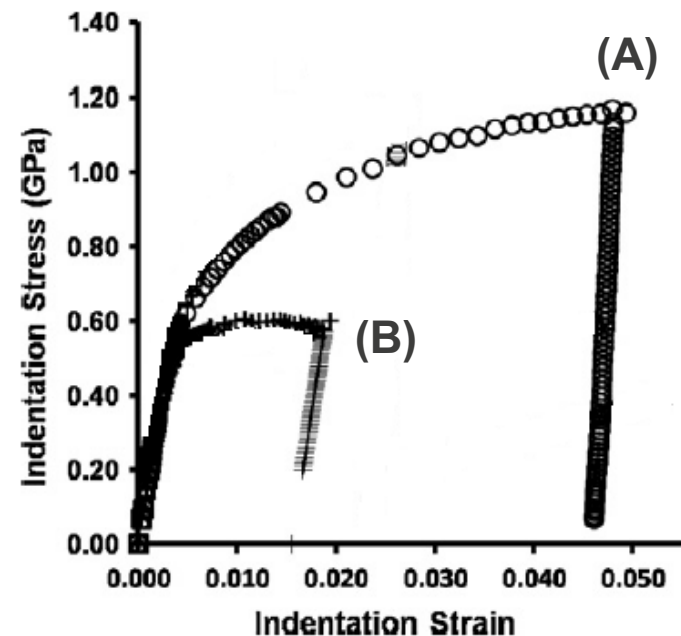
S. Basu et al. JMR, 2006.

$$(B) \quad \varepsilon_{ind} = \frac{4}{3\pi} \frac{h}{a}, \quad a = \frac{S}{2E_{eff}}$$

Kalidindi and Pathak. Acta Mat., 2008.

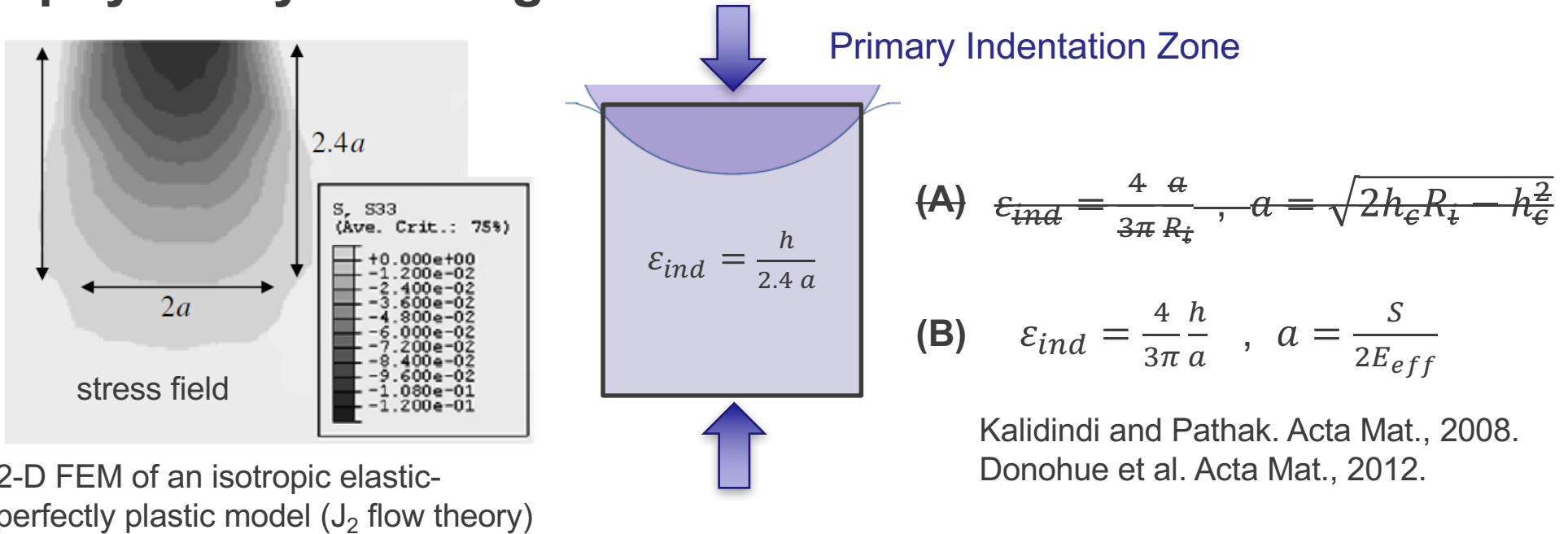
Donohue et al. Acta Mat., 2012.

Note: (A)=(B) for initial elastic loading



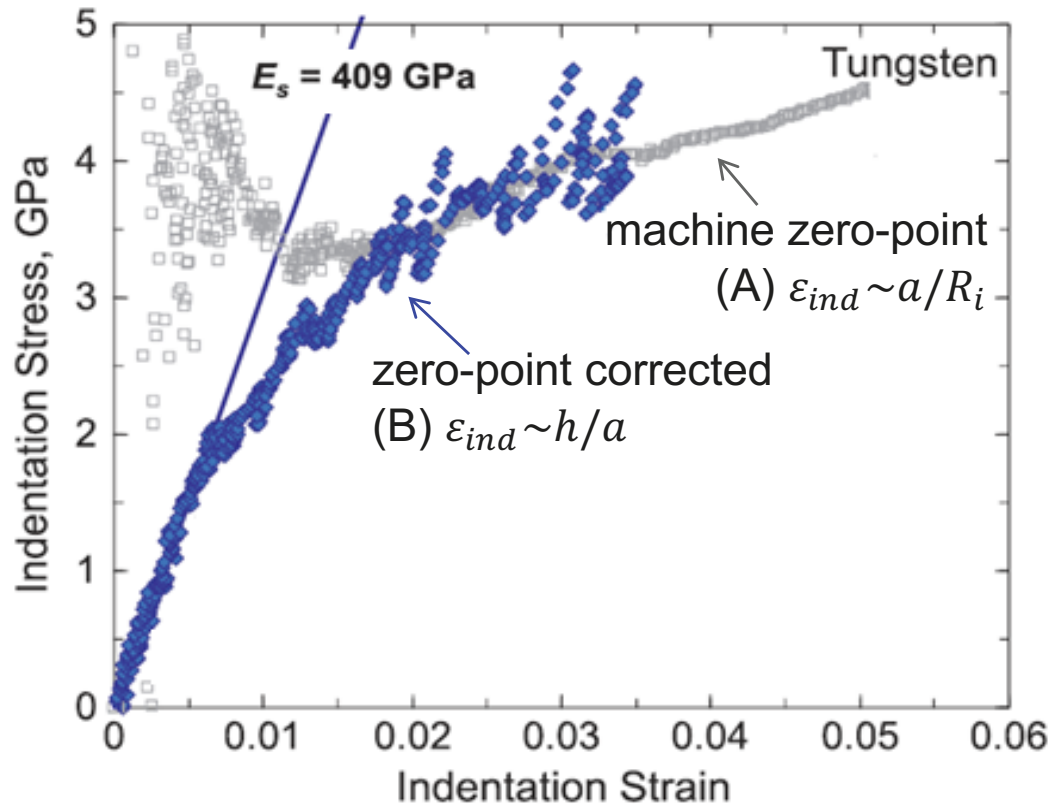
2-D FEM of an isotropic elastic-perfectly plastic model (J_2 flow theory)

The new definition of indentation strain is more physically meaningful



- Much closer to the average strain.
- Similar to compressing a cylinder with height $2.4a$ by displacement Δh .
- Fully consistent with Hertz's Theory.

An effective zero-point correction is required to recover the ISS curve



$$S = \frac{3(\tilde{P} - P^*)}{2(\tilde{h} - h^*)}$$

S : harmonic contact stiffness (CSM)
 \tilde{P}, \tilde{h} : machine load and displacement
 P^*, h^* : zero-point correction

- Deemphasizes tip and sample discrepancies.
- Indirectly corrects for tapping or “jackhammering” due to the CSM.

Addressing issues in nuclear materials with indentation stress-strain measurements

Previous work using these new protocols:

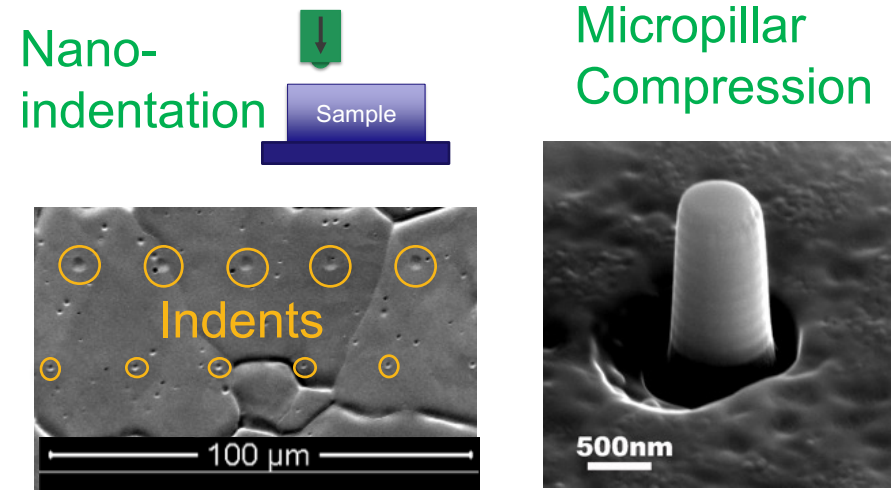
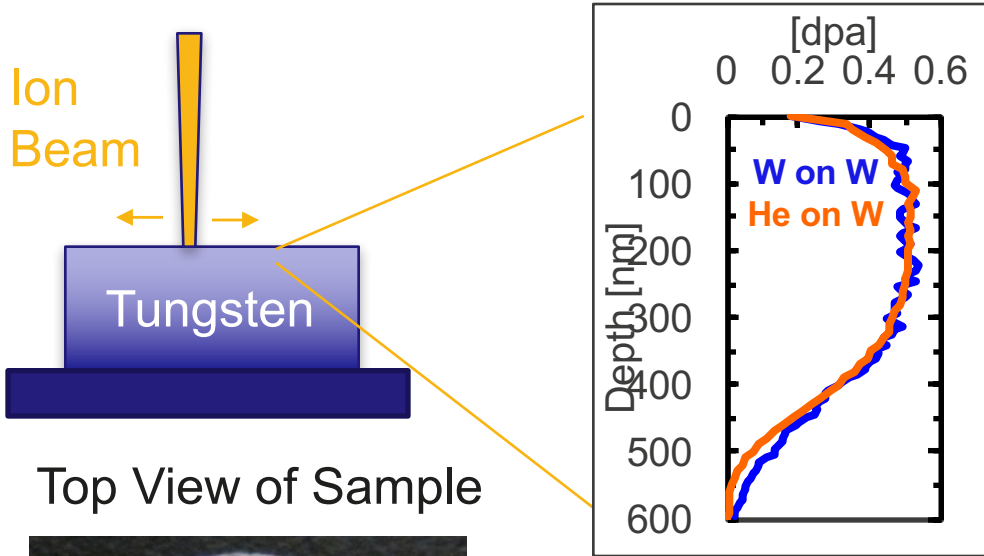
- Ideal systems (W, Al, Fe-3%Si).
- Focused on making grain scale measurements.
- Annealed or mildly deformed conditions.

Current work:

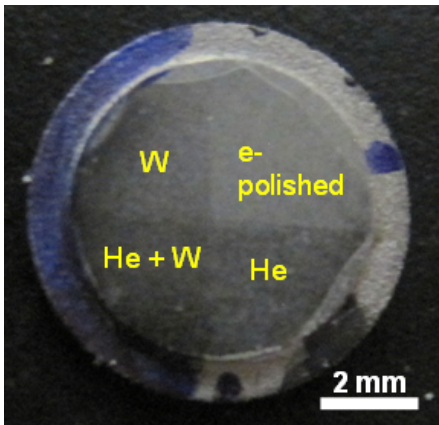
- More complex material systems (e.g. Zr, 304SS).
- Grain scale correlated to macroscopic or “bulk” length scales.
- Irradiated materials.
- Moving from metrology to material science – measuring new things.

Topic I: Irradiated Metals

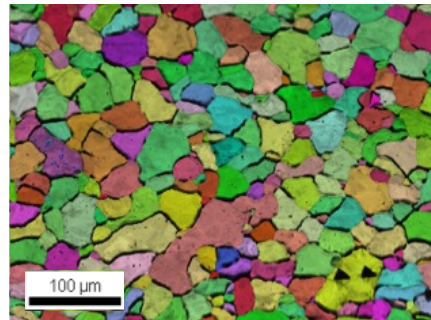
Indentation is high throughput tool for studying ion beam-induced radiation damage at the single grain level



Top View of Sample



EBSD-Orientation



Indenter radius, R	Indentation depth, h_t	Contact radius, a	Indentation zone $\sim 2.4a$
1 μm	~10 nm	60 nm	144 nm
5 μm	~14 nm	130 nm	312 nm
10 μm	~20 nm	250 nm	600 nm
100 μm	~40 nm	1,200 nm	2,880 nm
1000 μm *	>200 nm	12,800 nm	30,720 nm

ISS response of 'W on W' and 'He on W' are very different

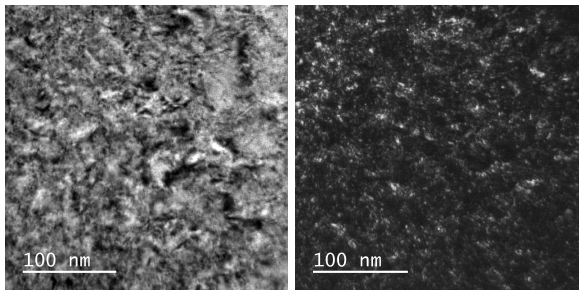
Unirradiated condition (annealed)

$E_s = 405$ GPa (isotropic)

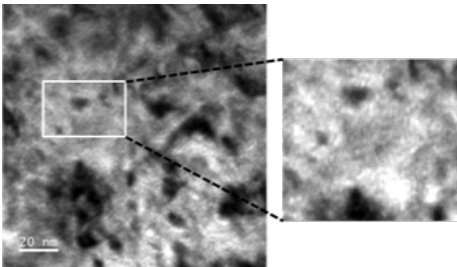
$Y_{ind} = 2.5$ GPa (100) - 3.0 GPa (111)

Dislocation loops ('W on W')

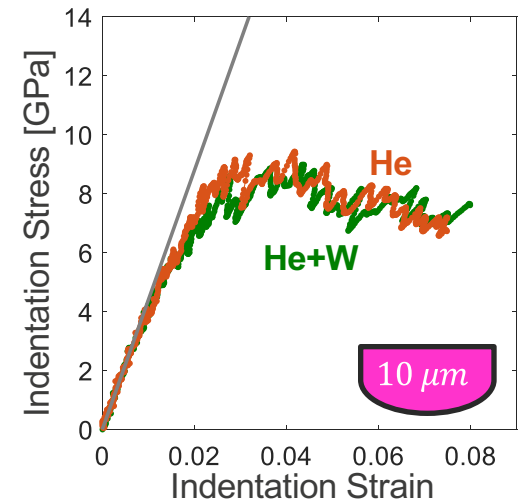
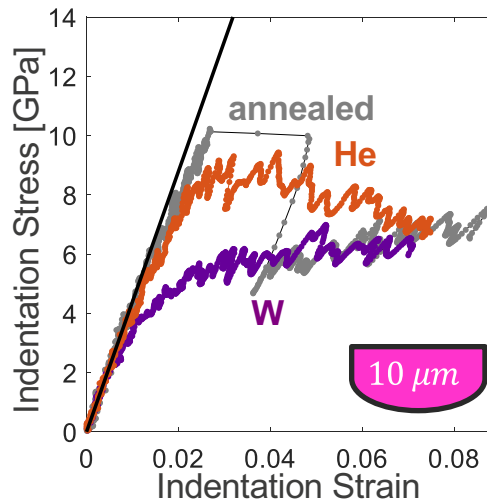
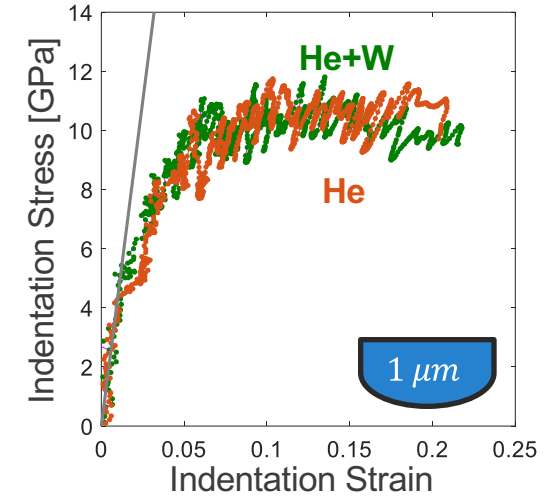
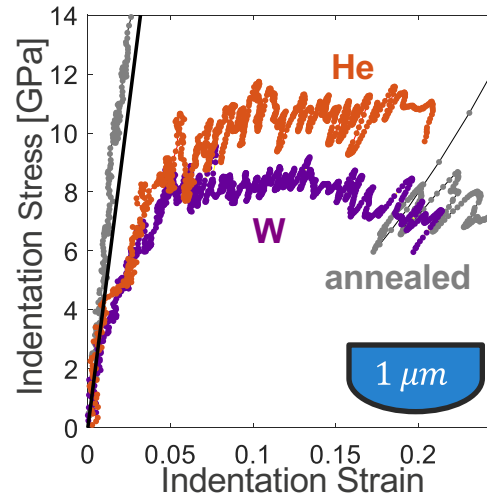
He bubbles + dislocation loops ('He on W')



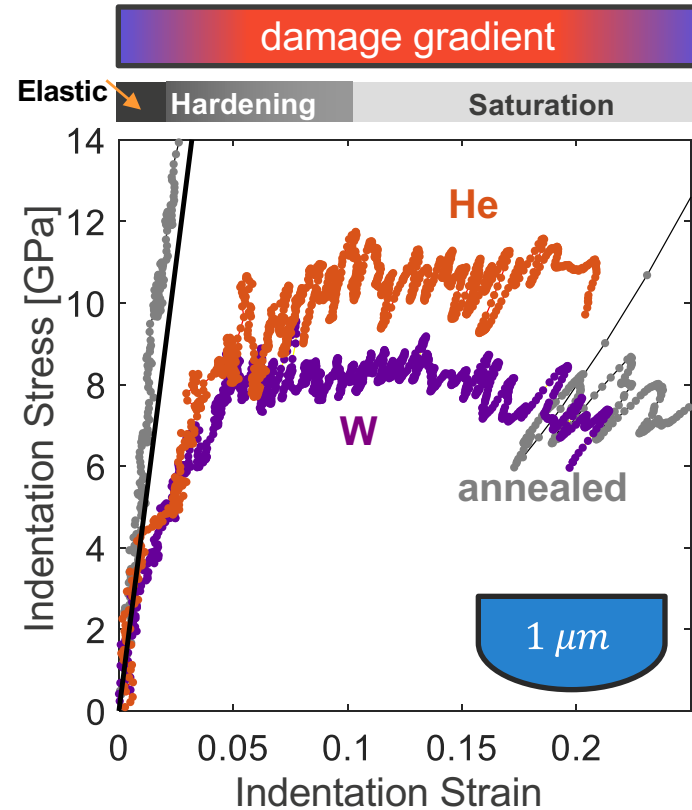
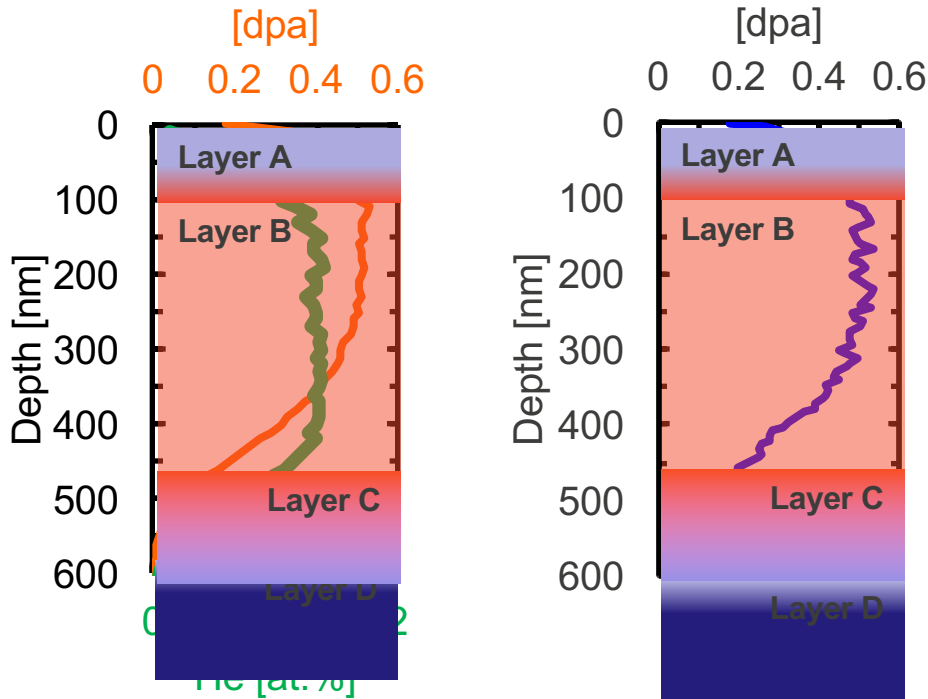
Dislocation loops



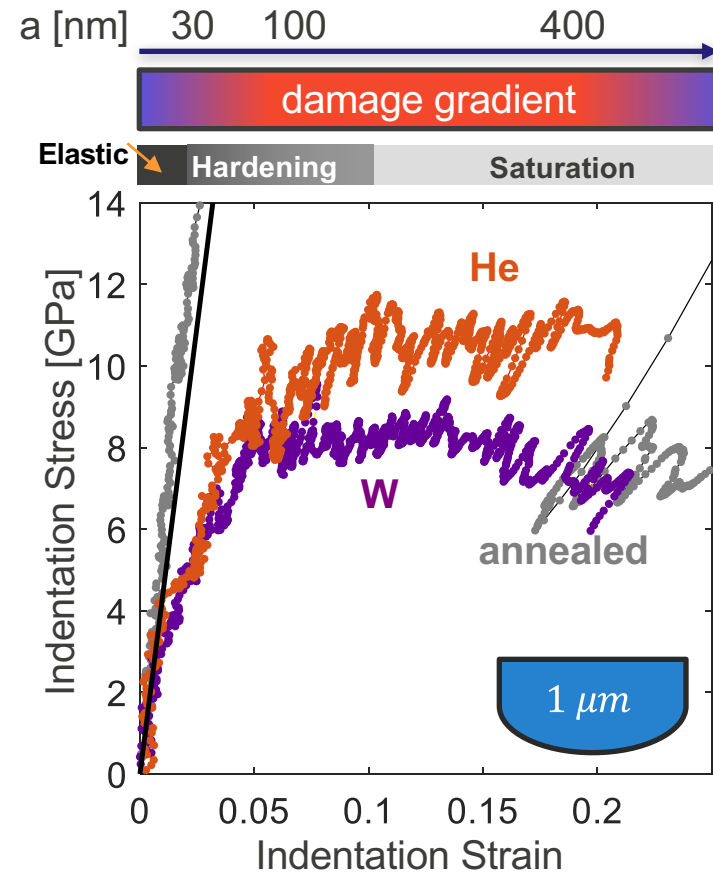
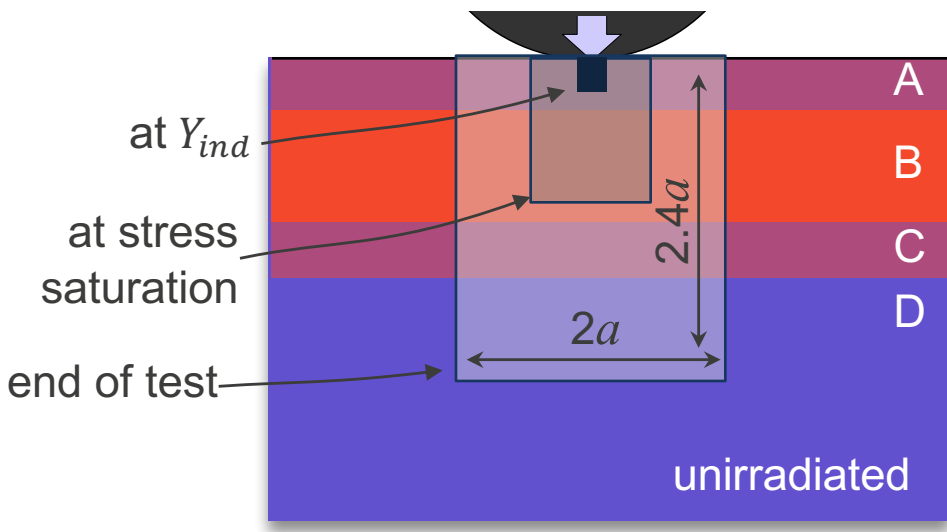
Helium bubble size: ~1.1 nm



The damage gradient matters for indentation measurements

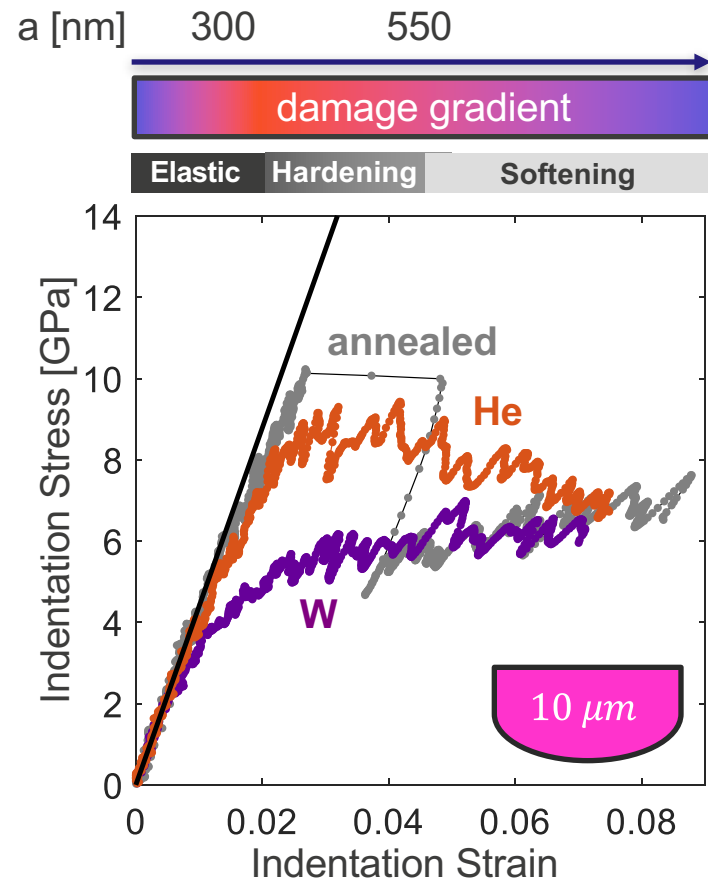
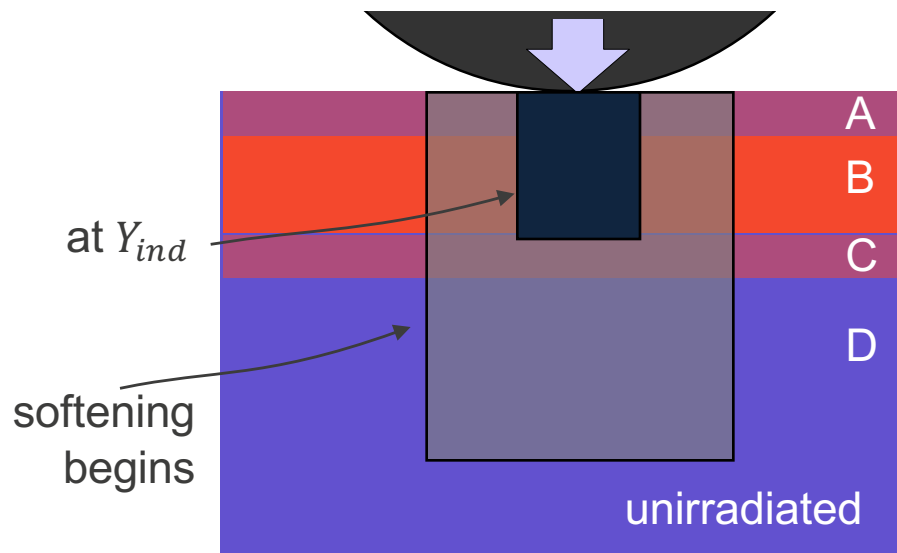


The saturation stress is likely the strength of the constant dose layer



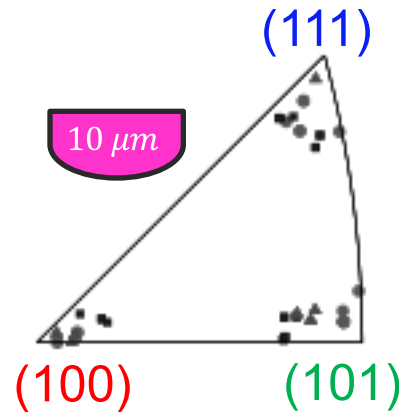
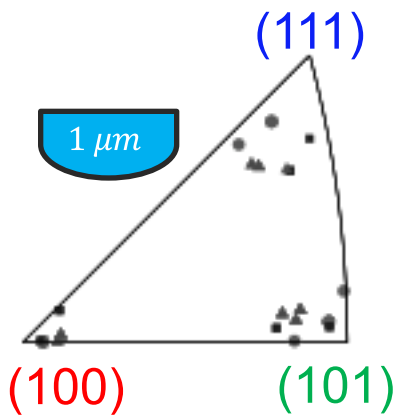
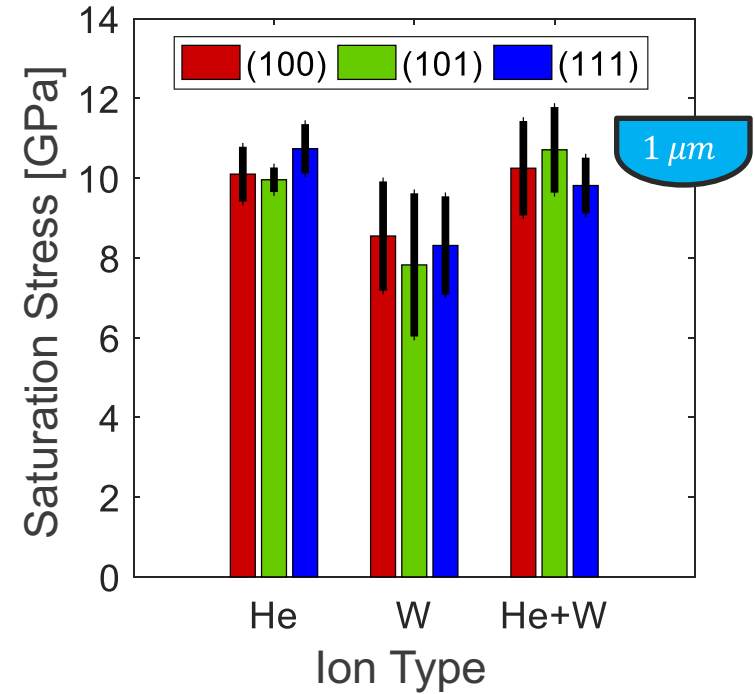
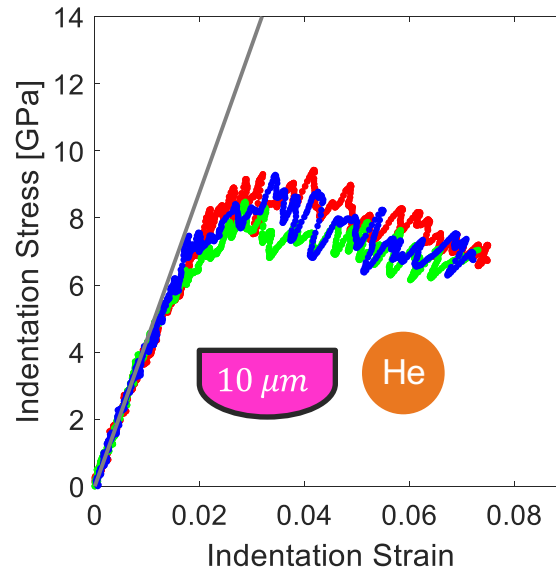
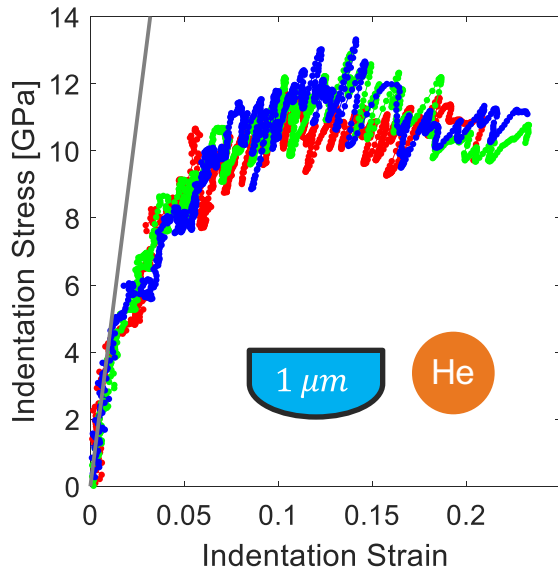
We can begin to validate and develop hardening models for different types of damage (He bubbles, dislocation loops, etc.)

Indentation can be used as a depth sensing probe



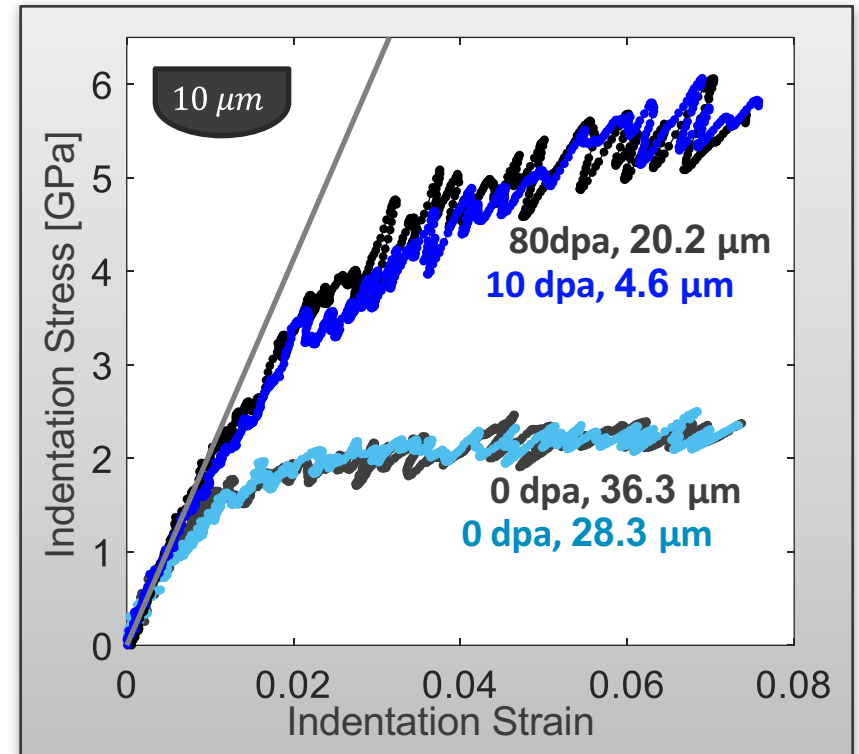
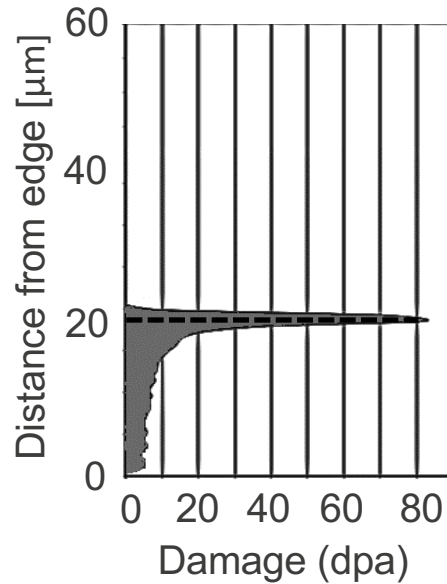
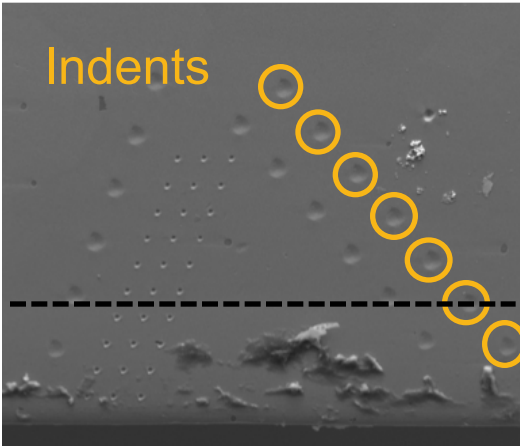
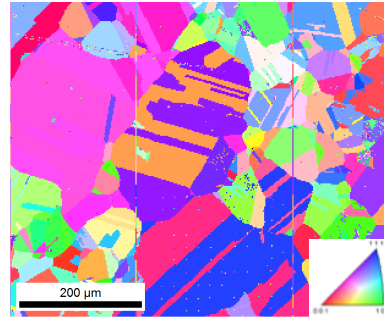
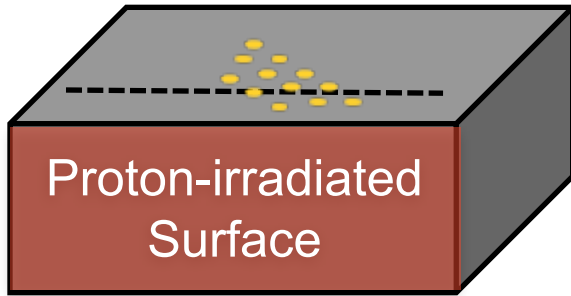
The peak stress (He) correlates well with the saturation stress from 1 μm tests.

The irradiated W material behaves plastically isotropic



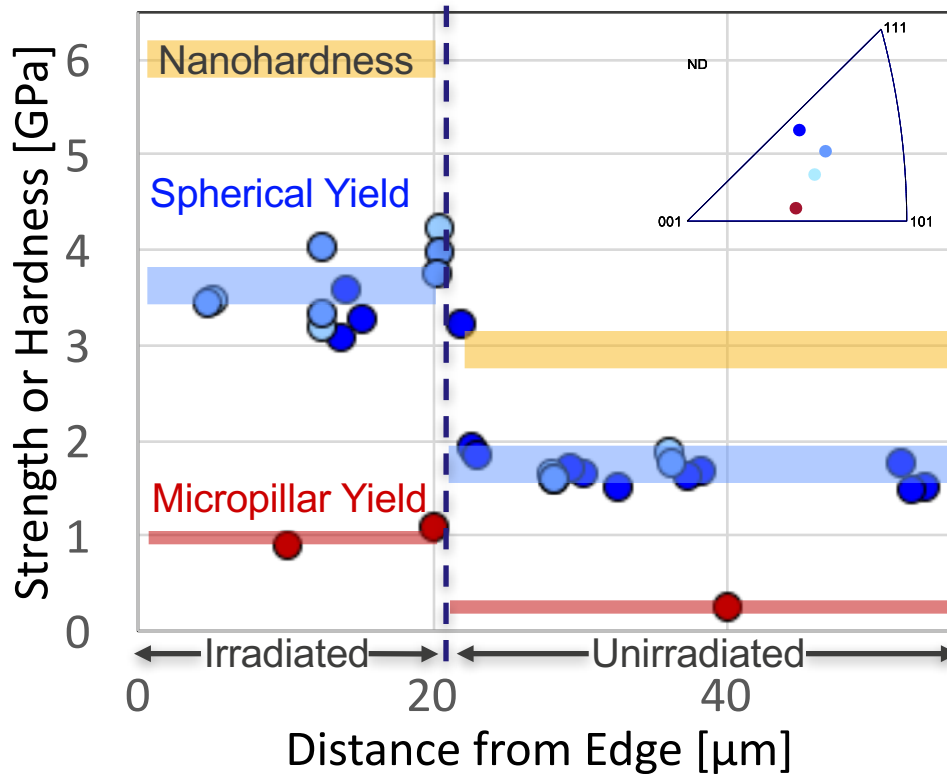
Ion Beam + EBSD + NI:
quickly explore crystal
orientation and ion type effects.

Proton-irradiated 304 stainless steel shows higher work hardening



High strength but also higher work hardening in the irradiated zone.

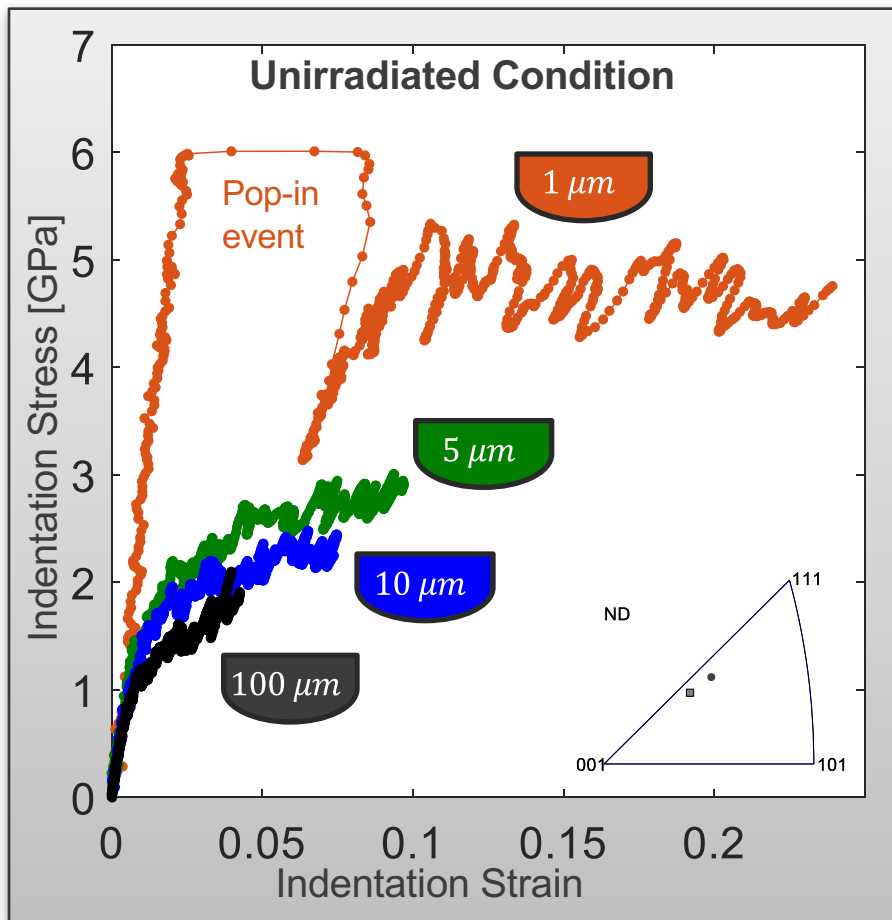
Benchmarking against other nano-mechanical tests shows differences between methods



	Nano-hardness	Spherical Yield	Micropillar Yield
Unirradiated Strength [GPa]	2.8	1.9	0.25
Irradiated Strength [GPa]	6.0	3.8	1.0
Strength Ratio	2.1	2.0	4.0
Contact radius/length [nm]	840	250	1,000

Both types of indentation measurements show ~2x lower ratio of strength between irradiated and unirradiated conditions compared to micropillar compression tests.

There is an indenter size effect in 304 stainless steel



- Higher work hardening in the irradiated compared to the unirradiated condition.
- Very different ratios of strength between irradiated and unirradiated conditions for indentation and micropillar compression tests.
- Indenter size effect (increasing strength with decreasing indenter size).

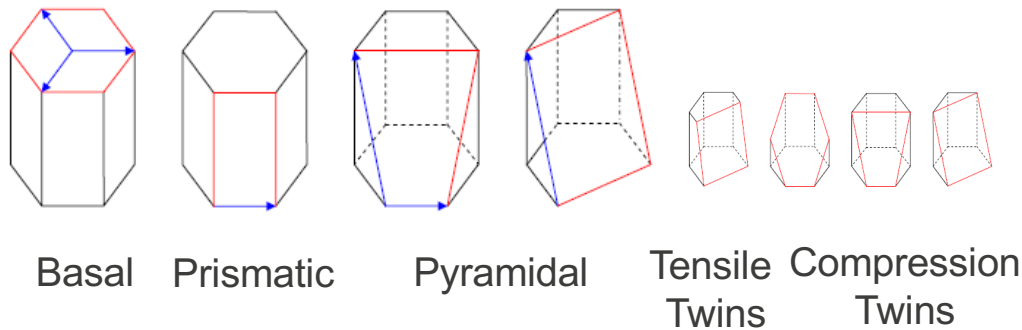
Martensitic phase transformation?

Ahn et al. Scripta Mat., 2010.

Ahn et al. Mat. Sci. Engr. A., 2014.

Topic II: HCP Metals

HCP metals are highly plastically anisotropic



Ti (c/a 1.588), CP and Ti-6Al

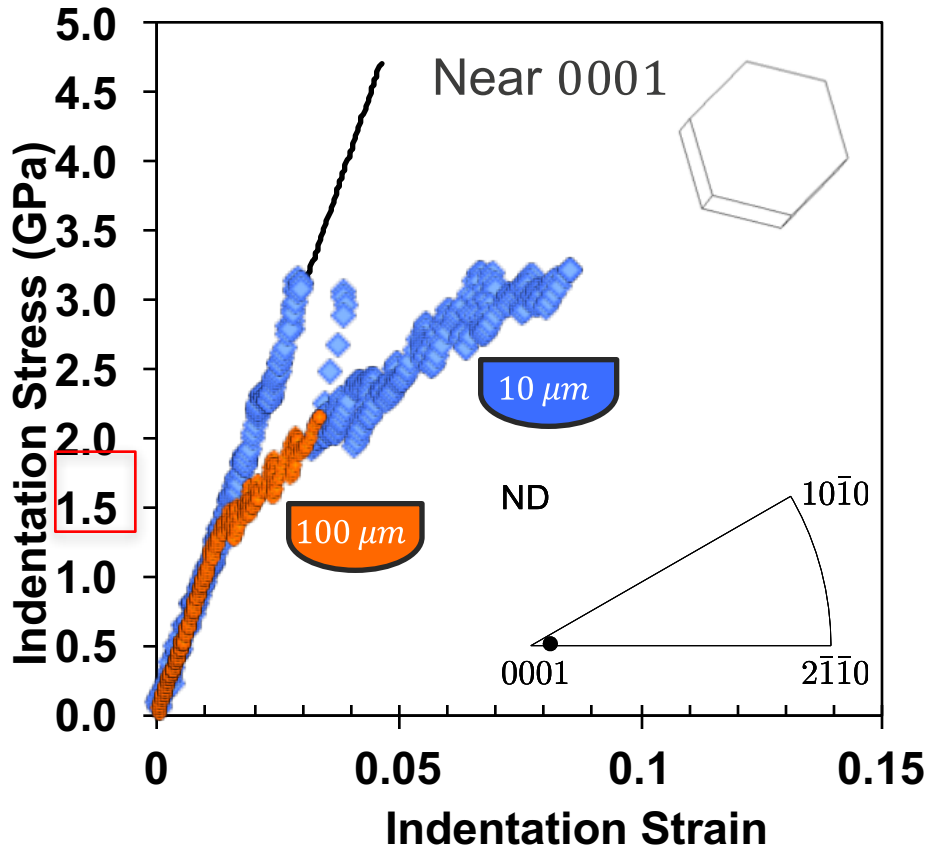
1-2x 1x 1.1-15x 10-15x

Zr (c/a 1.593), high purity

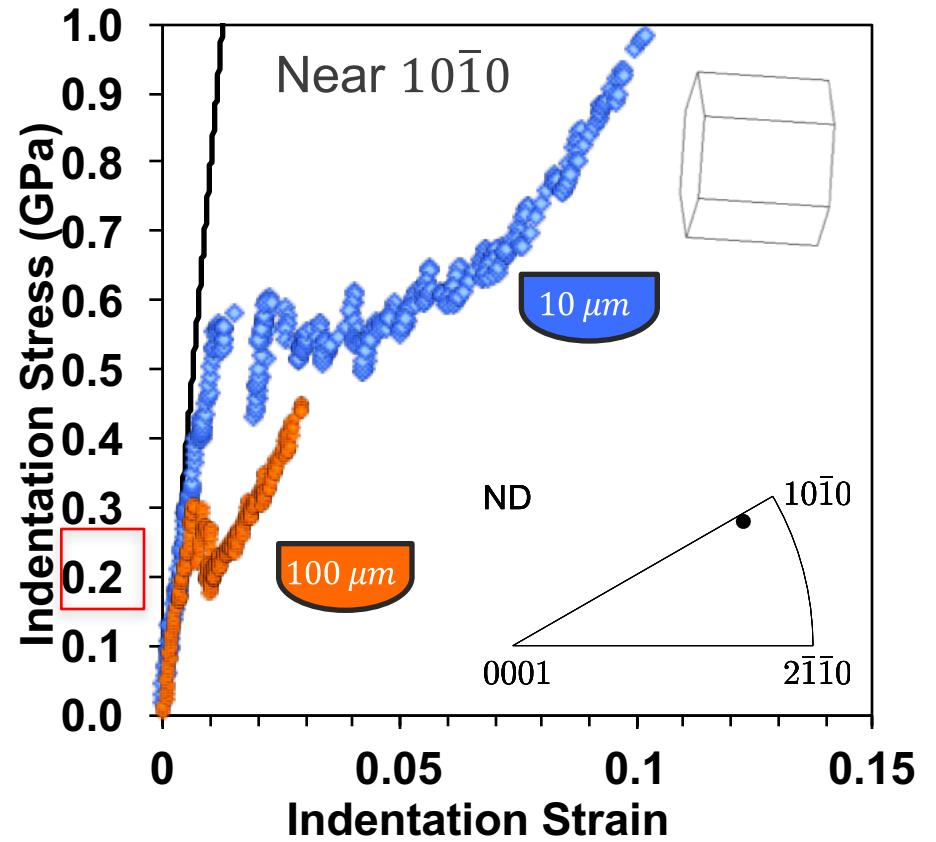
35x 1x 10x 1-10x 20x

- Slip resistances will depend on composition, temperature, etc.
- Such data is effort intensive (single crystals, micropillars, textured sheets).
- Can we reliably extract plastic parameters from indentation stress-strain curves?
- What degree of plastic anisotropy will the indentation stress-strain response show (Y_{ind})?

Indenter size effect in high purity zirconium



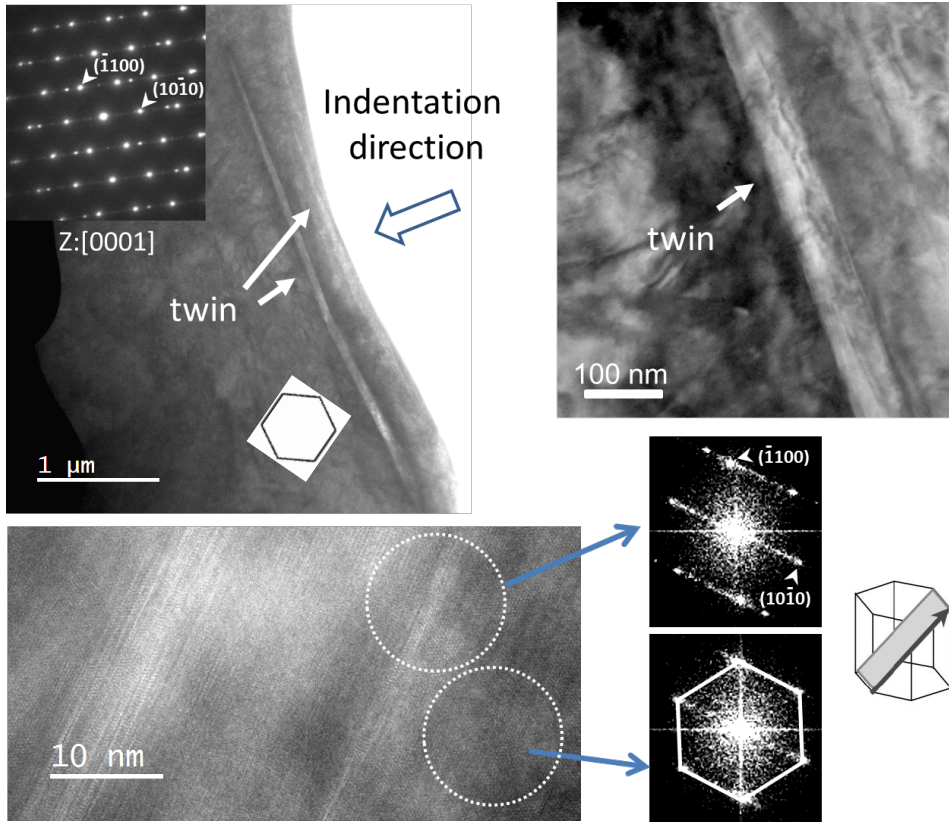
Constant high hardening



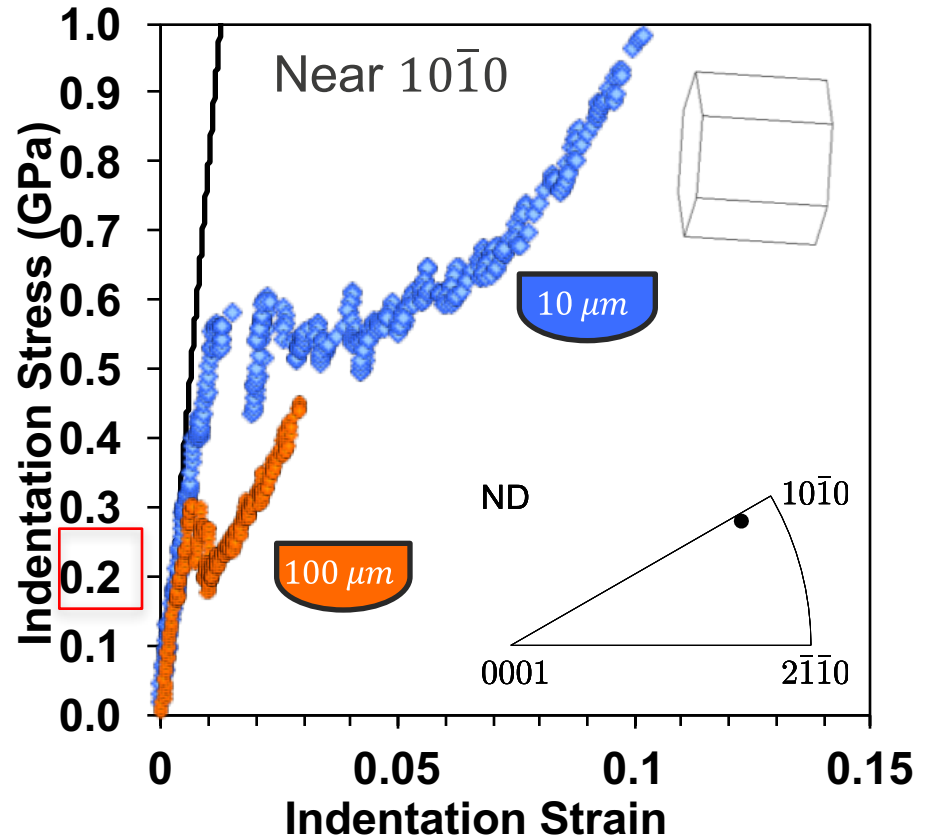
Sharp increase in hardening,
indenter size dependent

Extension twinning may be responsible for onset of steady-state work hardening

Near $10\bar{1}0$ 10 μm



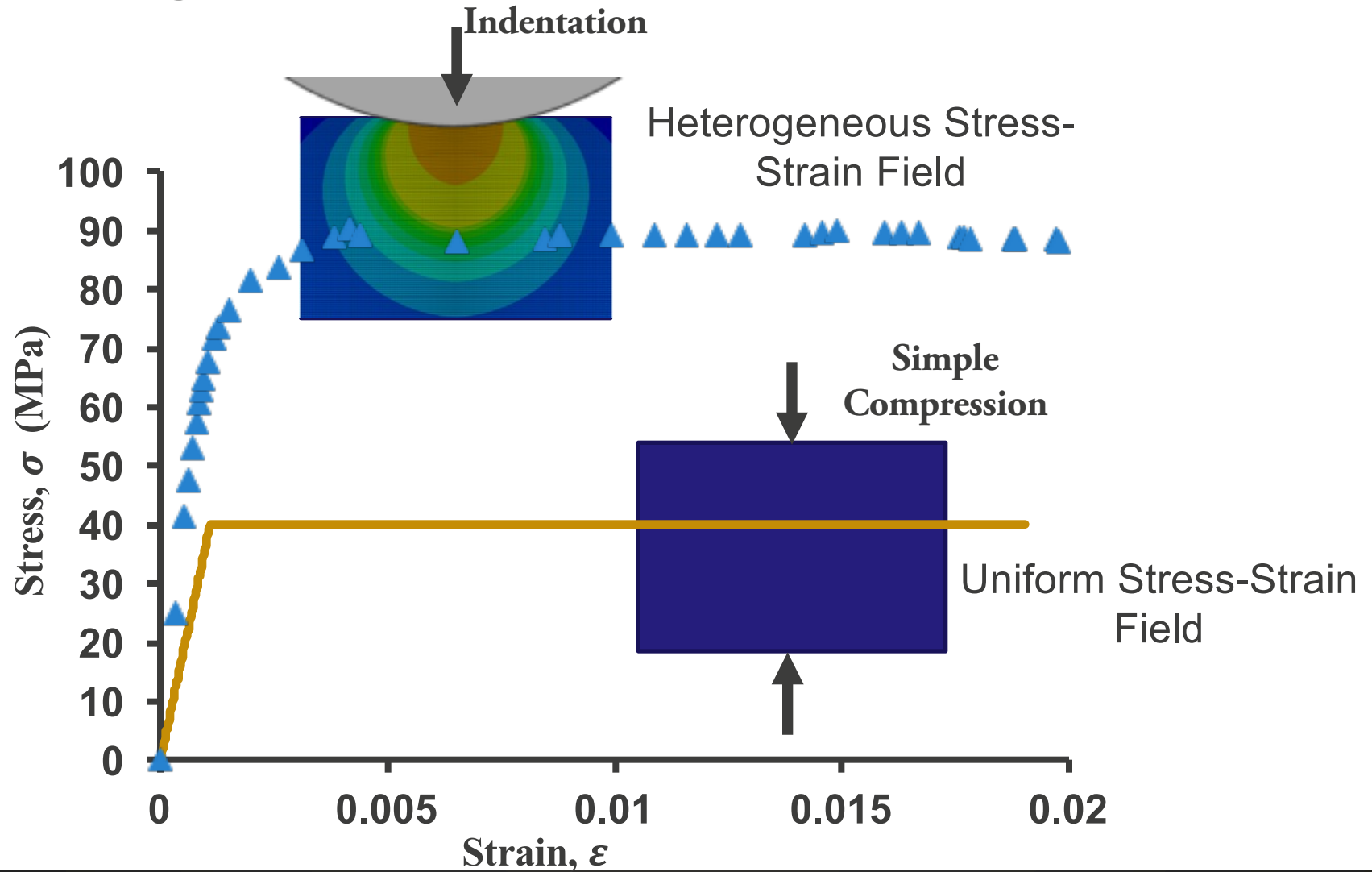
Courtesy of Cheng Sun



Critical contact radius 600-800 nm

Topic III: Correlation of indentation stress strain to uniaxial response

Correlating Indentation Stress-Strain to Uniaxial Stress-Strain



Correlating Indentation to Uniaxial Tests for Simple Materials

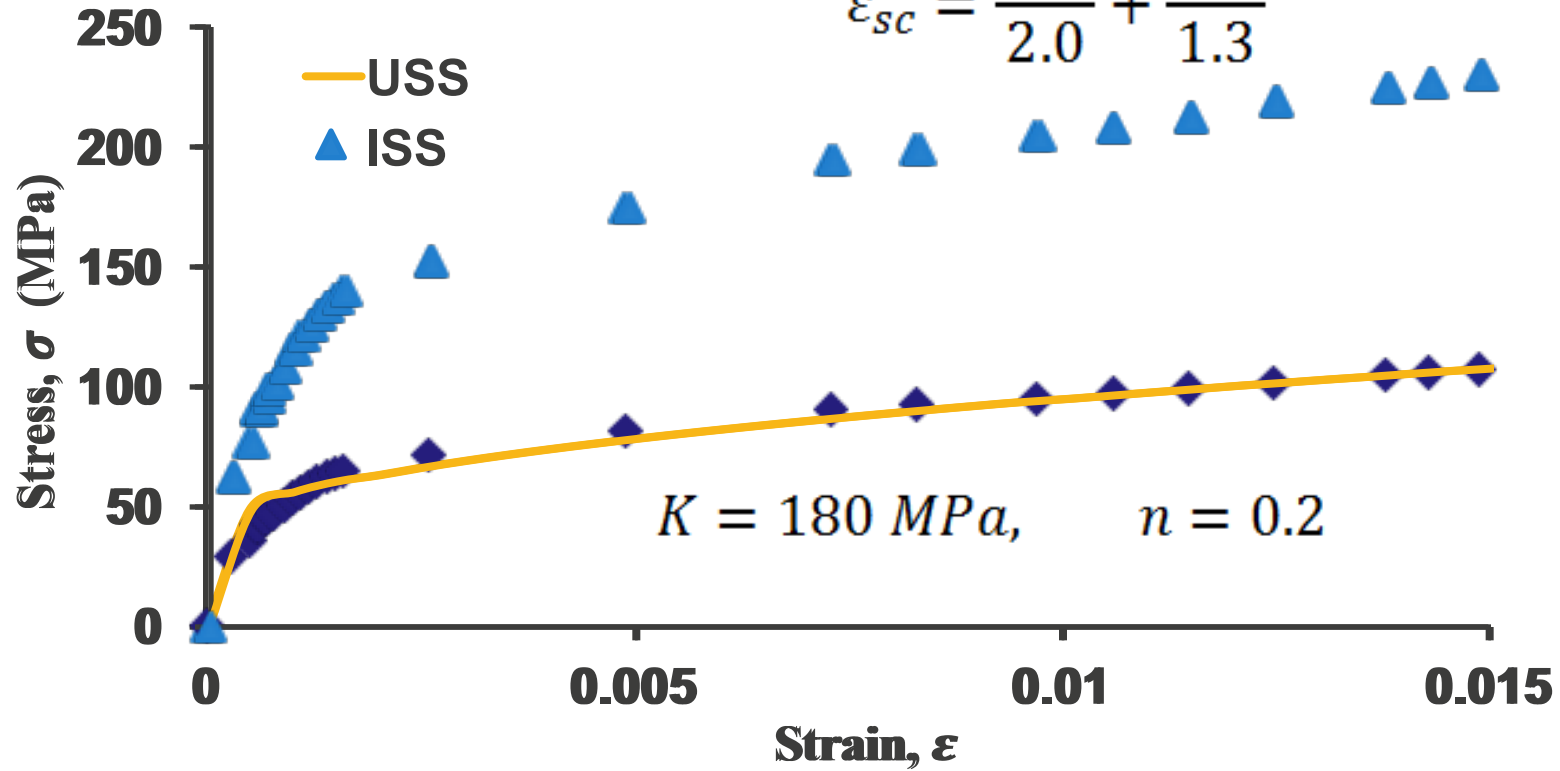
Scaling Stress

$$\sigma_{ind} \approx 2.20 \sigma_{sc}$$

Scaling Strain

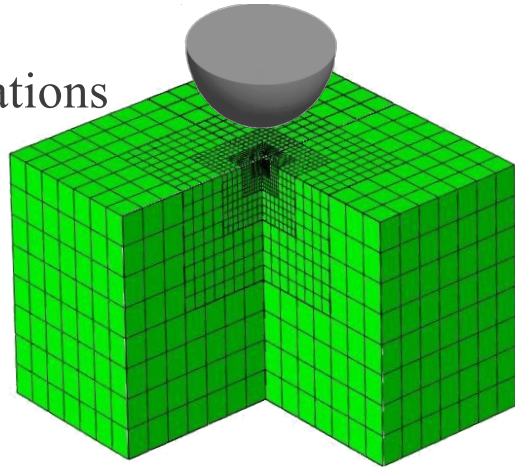
$$\epsilon_{ind} = \epsilon_{ind}^e + \epsilon_{ind}^p = \frac{\sigma_{ind}}{E_{eff}} + \epsilon_{ind}^p$$

$$\epsilon_{sc} = \frac{\epsilon_{ind}^e}{2.0} + \frac{\epsilon_{ind}^p}{1.3}$$



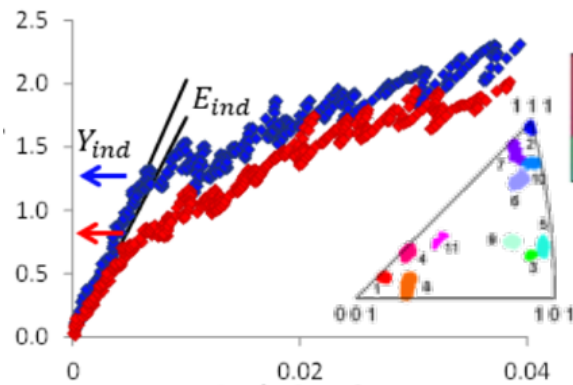
Extract Single Crystal Elastic-Plastic Properties

FE Simulations



+

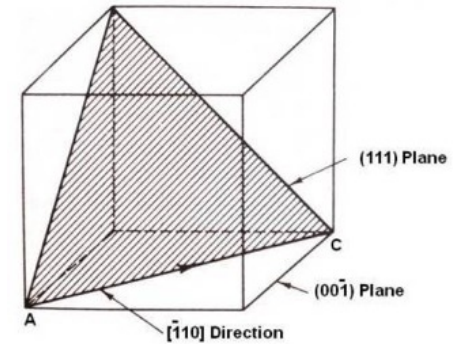
Experiments on Polycrystalline Sample



$$\sigma_{ij} = C_{ijkl} \epsilon_{kl}$$

$$C_{ijkl} = \begin{pmatrix} c_{11} & c_{12} & c_{12} & 0 & 0 & 0 \\ c_{12} & c_{11} & c_{12} & 0 & 0 & 0 \\ c_{12} & c_{12} & c_{11} & 0 & 0 & 0 \\ 0 & 0 & 0 & c_{44} & 0 & 0 \\ 0 & 0 & 0 & 0 & c_{44} & 0 \\ 0 & 0 & 0 & 0 & 0 & c_{44} \end{pmatrix}$$

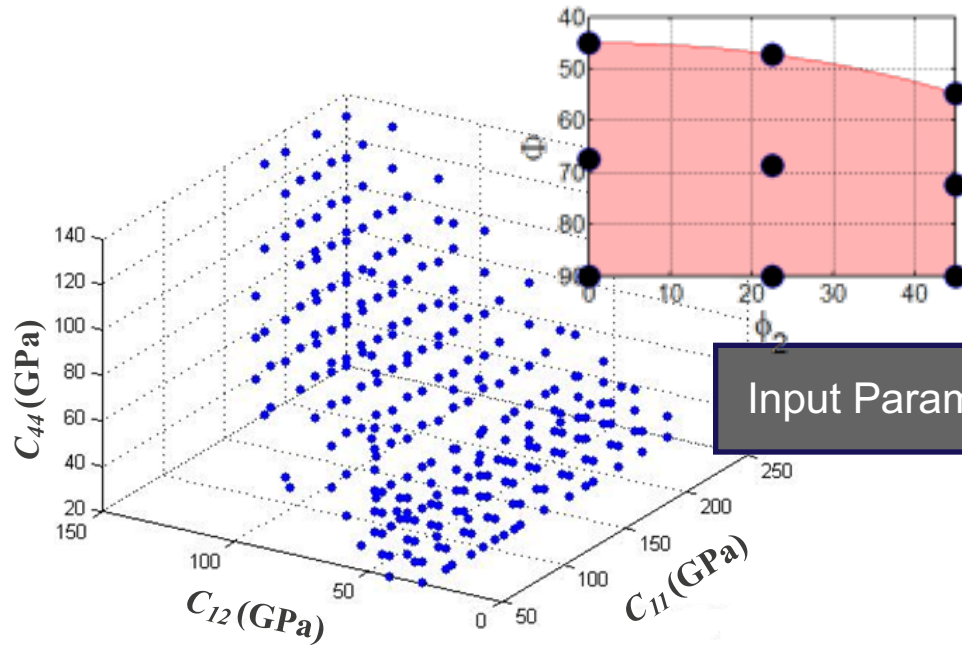
Elastic Stiffness Constants



Effective Slip Resistance

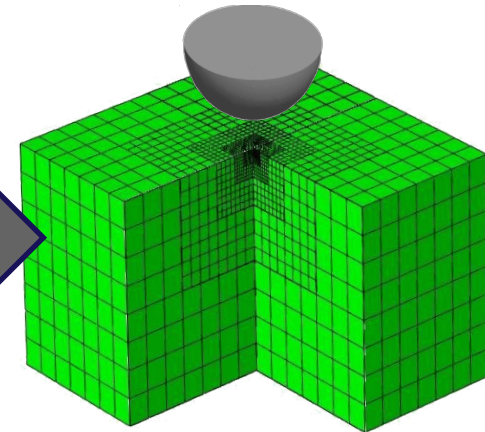
Spectral Representation of Indentation Modulus

Response database for **cubic** materials



Input Parameters

Finite Element Simulations

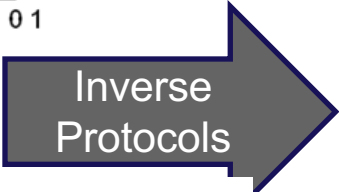
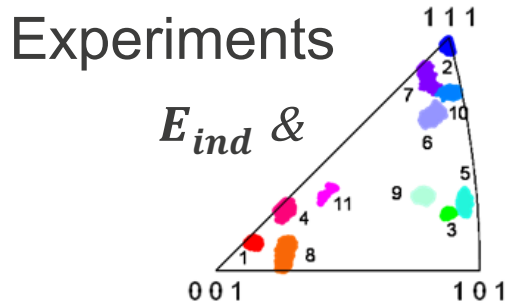


Functional Representation

$$E_{ind}(C_{11}, C_{12}, C_{44}, \Phi, \varphi_2) = \sum_{l=0}^{\infty} \sum_{m=1}^{M(l)} \sum_{q,r,s=0}^{\infty} A_l^{mqr s} \dot{K}_l^m(\Phi, \varphi_2) P_q(C_{11}) P_r(C_{12}) P_s(C_{44})$$

Extracting Single Crystal Elastic Stiffness Constants

Inverse Protocols



Single Crystal Elastic Constants for As-cast Fe3%Si

	C_{11} (GPa)	C_{12} (GPa)	C_{44} (GPa)
Literature*	225.28	131.68	123
Model Prediction	215.7	131.6	122.2

Prediction is within ~5% of the literature values

Functional Representation

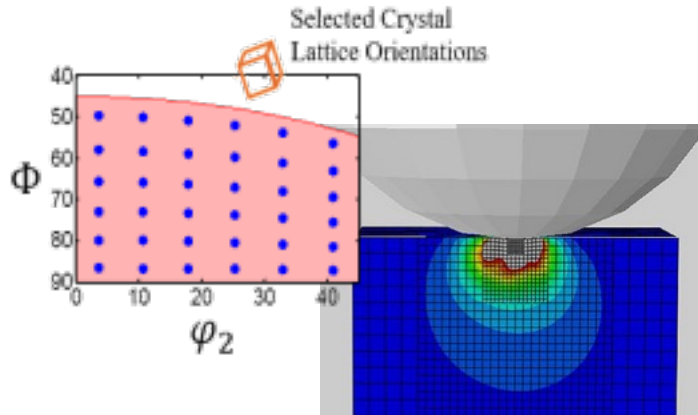
$$E_{ind}(C_{11}, C_{12}, C_{44}, \Phi, \varphi_2)$$

$$= \sum_{l=0}^{\infty} \sum_{m=1}^{M(l)} \sum_{q,r,s=0}^{\infty} A_l^{m q r s} \dot{K}_l^m(\Phi, \varphi_2) P_q(C_{11}) P_r(C_{12}) P_s(C_{44})$$

Patel, D.K., Al-Harbi, H.F., Kalidindi, S.R., 2014. Extracting single-crystal elastic constants from polycrystalline samples using spherical nanoindentation and orientation measurements. Acta Materialia 79, 108-116.

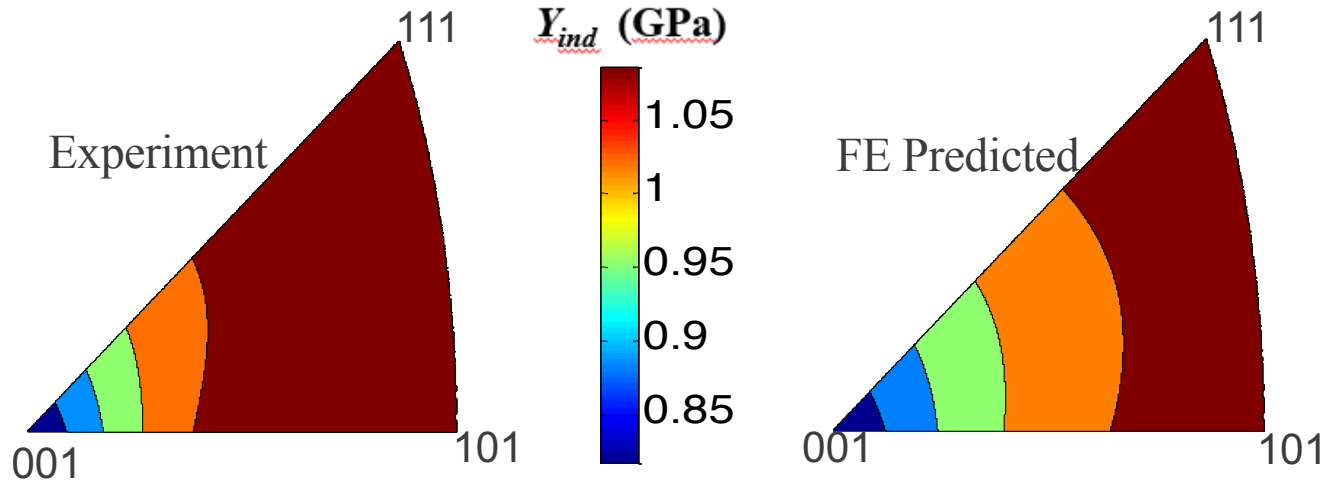
Orientation Dependence of Indentation Yield in BCC crystals

3D CPFEM Indentation Simulations



Spectral representation of indentation yield:

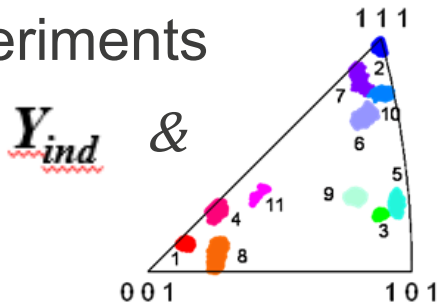
$$\tilde{Y}_{ind}(g) = \frac{Y_{ind}(g)}{s} = \sum_{l=0}^{\infty} \sum_{m=1}^{M(l)} B_l^m K_l^m(g)$$



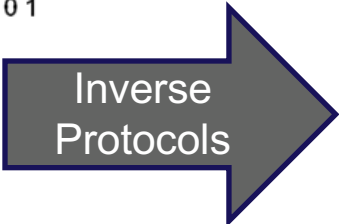
Case Study: As-cast Fe-3%Si polycrystalline BCC material

Protocols to estimate effective slip resistance parameter

Experiments



+



Effective slip resistance for As-cast Fe3%Si

	s (MPa)
Literature*	146.12 to 161
Model Prediction	155.4 ± 3.5

Functional Representation

$$\tilde{Y}_{ind}(g) = \frac{Y_{ind}(g)}{s} = \sum_{l=0}^{\infty} \sum_{m=1}^{M(l)} B_l^m K_l^m(g)$$

Prediction is within ~6% of the literature values

Patel, D.K. and Kalidindi, S.R. Estimating the slip resistance from spherical nanoindentation and orientation measurements in polycrystalline samples of cubic metals. IJP (Under Review)

Summary

- **Hardening models for irradiated materials under different irradiation conditions (e.g., W, 304SS)**
- **Grain scale mechanical property measurements including stresses for twinning and phase transformations (e.g., Zr, 304-SS)**
- **Fundamental basis for understanding the correlation between indentation stress-strain mode of deformation vs. uniaxial stress-strain**
- **Future work (through June 2017):**
 - Indentation Stress-Strain investigation of Zr, He, Zr+He implanted Zr
 - Gain Rad Protection approval to handle active samples in an upgraded indenter located in a radiological area
 - Indentation Stress-Strain investigation of reactor irradiated 304SS

